A mechanistic model (BCC-PSSICO) to predict changes in the hydraulic properties for bio-amended variably saturated soils

Albert Carles Brangarí,[1,2] Xavier Sanchez-Vila,[1,2] Anna Freixa,[3] Anna M. Romaní,[3] Simonetta Rubol,[4] and Daniel Fernàndez-Garcia[1,2]

Corresponding author: Albert C. Brangarí, Department of Civil and Environmental Engineering, Universitat Politècnica de Catalunya (UPC), Jordi Girona 1-3, 08034 Barcelona, Spain (albert.carles@upc.edu)

[1]Department of Civil and Environmental

Key Points.

- A new mechanistically-based model to estimate the impact of complex biofilms on the soil hydraulic properties.
- We derive a set of analytical equations for water retention and relative permeability.
- The model is corroborated by using real data from laboratory experiments and previously existing models.

Abstract. The accumulation of biofilms in porous media is likely to influence the overall hydraulic properties and, consequently, a sound understanding of the process is required for the proper design and management

Engineering, Universitat Politècnica de Catalunya (UPC), Jordi Girona 1-3, 08034 Barcelona, Spain.

[2]Associated Unit: Hydrogeology Group (UPC-CSIC).

[3]Institute of Aquatic Ecology, Department of Environmental Sciences, University of Girona, Campus Montilivi 17071 Girona, Spain.

[4]Department of Biological Sciences, Marine Environmental Biology Section, University of Southern California, Los Angeles, CA 90089, USA.

of many technological applications. In order to bring some light into this phenomenon we present a mechanistic model to study the variably saturated hydraulic properties of bio-amended soils. Special emphasis is laid on the distribution of phases at pore-scale and the mechanisms to retain and let water flow through, providing valuable insights into phenomena behind bioclogging. Our approach consists in modeling the porous media as an ensemble of capillary tubes, obtained from the biofilm-free water retention curve. This methodology is extended by the incorporation of a biofilm composed of bacterial cells and extracellular polymeric substances (EPS). Moreover, such a microbial consortium displays a channeled geometry that shrinks/swells with suction. Analytical equations for the volumetric water content and the relative permeability can then be derived by assuming that biomass reshapes the pore space following specific geometrical patterns. The model is discussed by using data from laboratory studies and other approaches already existing in the literature. It can reproduce i) displacements of the retention curve towards higher saturations and ii) permeability reductions of distinct orders of magnitude. Our findings also illustrate how even very small amounts of biofilm may lead to significant changes in the hydraulic properties. We therefore state the importance of accounting for the hydraulic characteristics of biofilms and for a complex/more realistic geometry of colonies at the pore-scale.

1. Introduction

The vadose zone is of major interest because of its role in the environment and in human life [*Selker et al.*, 1999]. The reason why the unsaturated zone is so appealing is that it connects different environmental compartments providing water and nutrients to the biosphere. As a result of this interaction, a wide range of bio-mediated processes with potential to modify soil characteristics are triggered [*DeJong et al.*, 2013].

In the middle of the twentieth century, engineers and soil scientists started paying attention to the significance of bio-mediated soil processes for the design and management of technological applications. One example where bioclogging has strong implications is the infiltration of water in recharge facilities, characterized by a pro-con dichotomy. On the one hand, the accumulation of biomass might be considered a disadvantage because it partially blocks flow paths [*Engesgaard et al.*, 2006; *Seki et al.*, 1998; *Vandevivere and Baveye*, 1992a; *Yarwood et al.*, 2006; *Zhong and Wu*, 2013], diminishing the efficiency of recharge ponds [*Baveye et al.*, 1998; *Pedretti et al.*, 2012], drainage fields [*Kennedy and Van Cuyk*, 2001], wetlands [*Knight et al.*, 2001; *Kadlec and Wallace*, 2008], and biofilters [*Mauclaire et al.*, 2006; *Soleimani et al.*, 2009]. On the other hand, the presence of bacterial communities has proved beneficial, as for example, it increases water retention time [*Van Cuyk et al.*, 2001], eventually facilitating the removal of contaminants [*Christensen et al.*, 2000; *Rodríguez-Escales et al.*, 2016; *Zhang et al.*, 1995]. Moreover, biomass driven permeability reduction may be exploited in geotechnical engineering [*Castegnier et al.*, 2006; *Ross et al.*, 2001], in CO_2 sequestration [*Cunningham et al.*, 2009], and in oil recov-

ery [*Abdel-Waly*, 2013]. Therefore, whether biomass accumulation proves to be an overall advantage or a drawback depends on the particular circumstances.

The largest and most diverse bacterial population in the biosphere coexists in the vadose zone [*Or et al.*, 2007a]. Many studies have pointed out the existence of large amounts of bacteria forming aggregates of cells [e.g., *De Beer and Schramm*, 1999; *Vandevivere and Baveye*, 1992a]. Most bacteria are embedded, to a greater or lesser extent, in a self-produced matrix forming biofilms attached to soil particles [*Fenchel*, 2002; *Young and Crawford*, 2004]. Such a matrix is composed of a combination of solids [*De Muynck et al.*, 2010; *Ehrlich*, 1999], gaseous by-products [*Rebata-Landa and Santamarina*, 2012; *Seki et al.*, 1998], and extracellular polymeric substances (EPS) [*Flemming and Wingender*, 2010; *Stoodley et al.*, 2002]. Moreover, biofilm comprises complex structures of intricate strandlike architecture that forms pores, voids and channels [*Stewart*, 2012; *Stoodley et al.*, 1994; *Wagner et al.*, 2010].

The accumulation of such a complex biomass in soils alters the pore geometry, and it is known to trigger significant changes in the hydraulic properties [*Bozorg et al.*, 2015; *Rockhold et al.*, 2002; *Or et al.*, 2007a]. However, it is difficult to correlate a given biofilm colonization with such changes. The capacity of microbial communities to dynamically adapt to the environmental conditions [*Kim et al.*, 2010; *Wilking et al.*, 2011] hampers the formulation of general models. This highlights the need for a sound understanding of the components and structure of the microbial community, as well as of their spatial distribution. A number of strategies with varying degrees of complexity have been adopted to evaluate the effects of biomass accumulation on the hydraulic properties. Some studies treat biofilm from a macroscopic point of view without assuming a specific pattern.

Clement et al. [1996] defined analytical expressions to account for porosity and permeability changes in saturated porous media. *Rockhold et al.* [2002] presented a composite media model in which these definitions were extended to unsaturated soils. *Rosenzweig et al.* [2012] explored the effect of EPS on the soil-water retention curve (SWRC) by using simple superposition. In contrast, some studies aim at describing biofilm and porous media in detail. Early studies modeled biofilm in saturated media as a continuous layer of uniform thickness covering the soil grains [*Rittmann*, 1993; *Taylor et al.*, 1990; *Cunningham et al.*, 1991] or as discrete microcolonies [*Vandevivere and Baveye*, 1992a]. *Mostafa and Van Geel* [2007, 2012] incorporated the presence of EPS and the distinction between active and inert biomass into the impermeable biofilm model. The permeability formulations were based on the approaches proposed by *Burdine* [1953] and *Mualem* [1976]. Meanwhile, *Thullner and Baveye* [2008] studied the use of biofilm layers embedded in cylindrical pores, and found that permeable biofilms growing in pore-networks are capable of simulating permeability reductions similar to the ones found in literature. Later on, Rosenzweig and coworkers focused on the effects of the distribution of impermeable biomass in unsaturated conditions. They assumed that biofilms cover the walls of cylindrical capillary tubes [*Rosenzweig et al.*, 2009] or of a pore-network consisting of triangular channels [*Rosenzweig et al.*, 2013, 2014]. Similarly, *Ezeuko et al.* [2011] and *Qin and Hassanizadeh* [2015] used geometries of increased complexity.

The present study provides a new mechanistic model that simulates the changes in the SWRC and the relative permeability induced by biofilm accumulation. Soil is represented as an ensemble of capillary tubes colonized by a complex biofilm. It is well known that this interpretation does not consider dual-occupancy or connectivity [*Likos and Jaafar*,

2013; *Beckett and Augarde*, 2013]; nevertheless, its use is quite standard in soil hydraulics [e.g., *Thullner and Baveye*, 2008; *Mostafa and Van Geel*, 2007; *Rosenzweig et al.*, 2009]. For the sake of simplicity it is used here as a first step towards a more realistic representation of biofilm complexity. The microbial phase in this model has six elements that are synthesized in the acronym PSSICO. Letter "P" stands for Porous, which indicates that the biomass matrix has an internal secondary porosity. "S" denotes Sticking, as we model only the biomass that grows attached to the solids, and not the one remaining in suspension. The second "S" implies that the microbial phase has Swelling properties, which changes volume and rheological properties in response to suction by absorbing/exuding water. "I" stands for Identifiable, denoting that the model requires a quantification of biomass from laboratory or field data, or estimated from a model. "C" is referred to the potential presence of biofilm Channels through which water can easily flow or be retained. Finally, "O" indicates that the biofilm is treated as a separate Object in a composite medium.

Using PSSICO, we developed a flexible theoretical model in an attempt to elucidate the mechanisms conditioning water retention and flow through bio-amended systems. Distinguishing between water in biofilms and in the pore-matrix, a set of analytical equations for saturation and relative permeability is derived. The model is used then to simulate the changes in the SWRC observed in two laboratory experiments. The results obtained are discussed and compared to other biofilm models from the literature. Finally, some conclusions are drawn from the sensitivity analysis of the parameters.

2. Conceptual Model

2.1. Water in Bio-amended Soils

Based on *Rockhold et al.* [2002], *Rosenzweig et al.* [2012], and *Taylor et al.* [1990], the accumulation of biomass leads to an increase in soil moisture for several reasons: i) the size and shape of the pore-matrix is altered by the accumulation of products, generating changes in the structure and connectivity of soils; ii) the biofilm contains a liquid phase mostly constituted by water; and iii) the wettability patterns of soils surfaces are modified. The total water content in bio-amended soils (θ_{tot}) may be defined as the sum of the volume associated with the microbial phase ($\theta_{w,bio} + \theta_{r,bio}$) and that of the pore-matrix ($\theta_{w,pm} + \theta_{r,pm}$),

$$\theta_{tot} = \theta_{w,bio} + \theta_{w,pm} + \theta_{r,bio} + \theta_{r,pm} = \theta_w + \theta_r, \quad (1)$$

where the subscripts r and w respectively determine whether water is in the residual state (irreducible) or not. The maximum value of θ_{tot} in (1) is equal to the porosity of the soil. Thus, when biofilm occupies the pore space it is at the expense of the portion initially available for open-pore water. The presence of biofilm components other than water (mainly solids particles), which would prevent the occurrence of full water saturation is neglected (details below).

2.2. Water in Biofilms

The complex structure and composition of biofilms [see *Flemming and Wingender*, 2010; *Or et al.*, 2007b; *Picioreanu et al.*, 2004] demands the use of a multifaceted definition of the microbial phase, which is achieved from the *six* elements of PSSICO. First, a proper Identification of the microbial phase is needed (component "I" in the model). Second, the treatment of the microbial phase in the literature has several interpretations. Some

authors treat it as a single unit [e.g., *Soleimani et al.*, 2009], whereas others stress the need to distinguish even between five types of microbial products [e.g., *Laspidou and Rittmann*, 2004]. In this paper we focus on the sticking ("S") biomass attached to soil grains, regardless of its origin (growth, reattachment, trapping or others). We disregard the biomass in suspension and soluble products that are less likely to modify hydraulic properties. Thus, biofilm consists of bacteria and EPS so that

$$M_{bio}(t) = M_{bact}(t) + M_{EPS}(t), \tag{2}$$

where M_{bact}, M_{EPS}, and M_{bio} are respectively the masses of bacteria, EPS, and total biofilm, expressed in grams of dry mass per unit volume. The time variable (t) denotes that biofilm composition may change with time.

Concerning its structure, biofilms can be seen as a complex three-dimensional network of strands of EPS and bacteria forming voids and channels (Figure 1). Such structure has significant implications in the way biofilm interacts with water; actually it behaves like a sponge with a large absorbing capacity that shrinks/swells with suction changes ([*Or et al.*, 2007b]). Under fully hydrated conditions the EPS-dominated matrix can hold up to 70 times its weight in water [*Chenu*, 1993]. On the contrary, biofilms respond by shrinking when suction increases becoming dense and amorphous, albeit holding a considerable amount of water. Such a mechanism enhances dehydration resistance and fast recovery swelling after desiccation [*Tamaru et al.*, 2005], minimizing the impact of dry conditions upon bacterial life [*Or et al.*, 2007b].

According to *de Gennes* [1979], the equilibrium mass ratio between a polymer and water may be defined by a power-law of suction; assuming further that only the EPS behaves

like a polymer, the volume of mobile water in biofilms is estimated by

$$\theta^*_{w,bio}(\psi, M_{bio}) = \frac{M_{EPS}}{\rho_w} A\psi^{-B}, \tag{3}$$

where ψ is the matric suction (in cm), ρ_w the density of water, and A, B are fitting experimental parameters. *Rosenzweig et al.* [2012] found values of $A = 105.76$ and $B = 0.489$ for pure xanthan ($C_{35}H_{49}O_{29}$), a natural polysaccharide widely used as an EPS analog [*Chenu*, 1993; *Rosenzweig et al.*, 2012]. Nevertheless, the hydraulic properties of EPS depend on its specific composition. Particularly, xanthan depicts an outstanding retention capacity that is larger than other polysaccharides such as scleroglucan or dextran [*Chenu*, 1993]. Our model can effortless incorporate other type of relations (general or specific for a given study case) since it is not limited by working assumptions in (3-7).

The boundless behavior of $\theta^*_{w,bio}$ when ψ approaches zero demands the imposition of some restrictions in (3) that indirectly limits the volumetric density of biofilms. The maximum amount of water kept by biofilm is defined equal to 70 times its own mass [based on *Chenu*, 1993], and it is also limited by the effective porosity (ϕ_{ef}). Thus, we can provide the following water in biofilms in pores to calculate applying such thoughts as

$$\theta_{w,bio}(\psi, M_{bio}) = min\left(\theta^*_{w,bio}, 70\frac{M_{bio}}{\rho_w}, \phi_{ef}\right). \tag{4}$$

On the other hand, it seems logical to link $\theta_{r,bio}$ to the composition of the biofilm. From the contributions of bacterial cells and EPS we obtain

$$\theta_{r,bio}(M_{bio}) = 0.8\frac{M_{bact}}{\rho_w} + \frac{M_{EPS}}{\rho_s}\theta_{r,EPS}, \tag{5}$$

where ρ_s is the bulk dry soil density and $\theta_{r,EPS}$ the residual water content for pure EPS. The first term in (5) considers the volume retained inside the body of bacteria. Water in cells is considered fully irreducible regardless of the environmental conditions, and it

is here quantified as 80% of the cellular volume [*Cooke and Kuntz*, 1974]. The remaining volume is neglected. The second term in (5) accounts for water in the polymeric matrix. The lack of information is overcome by assuming that under oven-dry suction the EPS can hold as much water as a clay material [inspired from *Peña-Cabriales and Alexander*, 1979; *Rockhold et al.*, 2002], $\theta_{r,EPS} \equiv \theta_{r,clay}$. Such a value is available in the literature [e.g., *Carsel and Parrish*, 1988], albeit it still displays high variability among studies.

2.3. Water Flow through Biofilms

Technological advances in instrumentation have demonstrated that water flows through biofilms [*Billings et al.*, 2015]. Besides the intrinsic permeability of biological materials, void structures act as preferential flow paths that confer significant permeability to the biofilm [*Davit et al.*, 2013; *De Beer and Schramm*, 1999; *Lawrence et al.*, 1991]. Therefore, the flow capacity depends on both the structure and composition of the biofilm constituents. We simply assume here that the water flowing through biofilms has a dynamic viscosity (μ_{bio}) different from that in the pore-matrix (μ_w) [as in *Qin and Hassanizadeh*, 2015; *Pintelon et al.*, 2012; *Thullner and Baveye*, 2008]. This hypothesis, which was first proposed by *Dupin et al.* [2001], states that

$$\mu_{bio}(\psi) = \lambda_\mu(\psi)\mu_w, \tag{6}$$

where λ_μ (always greater or equal to 1) specifies the increased resistance of water flowing through biofilm. Since there are no specific studies on the effect of shrinking/swelling in λ_μ, we postulate the following expression

$$\lambda_\mu = \frac{1}{1 - \left[\dfrac{\theta_{r,bio}}{\theta_{w,bio} + \theta_{r,bio}}\right]^\eta}, \tag{7}$$

where η is a dimensionless parameter accounting for the stiffness of the viscous variation effect. The smaller the value of η, the more impermeable the biofilm. Figure 2 shows that when $\theta_{w,bio}$ is very high with respect to $\theta_{r,bio}$, the microbial phase is diluted and λ_μ tends to 1. When $\lambda_\mu = 1$ the water contained in biofilms flows as in the pore-matrix. In contrast, when biofilm shrinks and becomes denser, λ_μ increases tending to infinity.

3. The BCC-PSSICO Model

3.1. The Retention Curve of a Bio-amended Soil

Based on the capillary tube analogy, soil pores are replaced by a bundle of cylindrical capillaries (BCC) of different diameters. Let $f(r_0)$ be the frequency distribution of pore radii associated with a biofilm-free soil so that $f(r_0)dr_0$ is the number of capillary tubes per unit area with radii ranging between r_0 and $r_0 + dr_0$ before any biofilm is formed. We assume that the largest water-filled capillary tube available at a given matric suction ψ_0, denoted as R_0, is obtained from the capillary rise equation

$$\psi_0 = \frac{2\sigma \cos(\beta)}{R_0 \gamma_w}, \tag{8}$$

where σ is the surface tension, β the contact angle and γ_w the specific weight of water. Then, the open-pore water content of a biofilm-free soil may be written as

$$\theta^0_{w,pm}(R_0) = \int_{R_{0,min}}^{R_0} \pi r_0^2 f(r_0) dr_0, \tag{9}$$

yielding

$$f(r_0) = \frac{2\sigma \cos(\beta)}{\gamma_w \pi r_0^4} \frac{d\theta^0_{w,pm}}{d\psi_0}, \tag{10}$$

where $R_{0,min}$ is the minimum pore radius. This value may be estimated from (8) using the maximum soil suction, which is generally considered in the order of 10^5 m [e.g., *Mitchell and Soga*, 2005]. The term $d\theta^0_{w,pm}/d\psi_0$ is the derivative of the SWRC expression. Despite

many alternatives can be used [e.g., *Brooks and Corey*, 1964], the van Genuchten equation (11) and its derivative (12) are simple, continuous and match the SWRC for a variety of soils by using only two fitting parameters (n and α) [*van Genuchten*, 1980].

$$\theta^0_{w,pm}(\psi_0) = \phi_{ef}\left[1 + [\alpha\psi_0]^n\right]^{\frac{1}{n}-1} \tag{11}$$

$$\frac{d\theta^0_{w,pm}(\psi_0)}{d\psi_0} = \alpha\phi_{ef}[1-n][\alpha\psi_0]^{n-1}\left[1 + [\alpha\psi_0]^n\right]^{\frac{1}{n}-2} \tag{12}$$

However the presence of biomass reshapes the open porosity with the result that the content of open-pore water becomes

$$\theta_{w,pm}(R) = \int_{R_{min}}^{R} \pi r^2 f(r) dr, \tag{13}$$

where $f(r)$ is the new pore-size distribution of the bio-amended soil. The matric suction at which the transformed tube radius empties is still given by the capillary rise equation, written now as

$$\psi = \frac{2\sigma\cos(\beta)}{R\gamma_w}. \tag{14}$$

Then, the relation between (8) and (14) may be expressed as

$$\psi = \frac{\psi_0}{X}, \tag{15}$$

where X is a parameter that will be defined and discussed below.

The spatial competition between open-pore water and biofilm is illustrated in Figure 3. Note that when $\psi = \psi_{max}$, the volume of water in the biofilm is minimum (residual) and $\theta_{w,bio} = 0$; but it rises as suction decreases, modifying the open porosity. The characteristics of the new pores depend on how biomass reshapes the capillary tubes. Some previous studies consider that biofilm forms a layer attached to the pore walls [e.g. *Ezeuko et al.*, 2011; *Mostafa and Van Geel*, 2007; *Rosenzweig et al.*, 2009]. The distribution patterns of this biofilm depend on whether it grows preferentially either in the smaller or

in the larger pores, or uniformly in all of them [see the lucid discussions in *Bundt et al.*, 2001; *Mostafa and Van Geel*, 2007; *Rosenzweig et al.*, 2009]. Although the distribution and morphology at the pore-scale is still an unresolved challenge, from the experimental evidence (see Figure 1) we consider that biofilms bring about changes in the pore-size distribution according to two mechanisms:

(i) the number of capillary tubes per unit soil area between r_0 and $r_0 + dr_0$ increases by a factor N so that

$$f(r)dr = Nf(r_0)dr_0, \tag{16}$$

(ii) the new tube radii are reduced by a positive real factor $X(\leq 1)$ with the result that

$$r = Xr_0. \tag{17}$$

Such a new combination of mechanisms allow the biofilm to show a relatively flexible architecture since it may be partially detached from the walls being located in the middle of the tubes cross-section. From a practical standpoint, this means that every single tube of radius r_0 is converted into N equal cylindrical tubes of radius r, reproducing structural channels embedded in the biofilm matrix. The effect of this transformation may be observed in Figure 4.

Substituting (16) and (17) into (13), we have

$$\theta_{w,pm}(R) = NX^2 \int_{R_{0,min}}^{R_0} \pi r_0^2 f(r_0)dr_0 = NX^2\theta^0_{w,pm}(R_0), \tag{18}$$

where, from (15), the pore-matrix water content is

$$\theta_{w,pm}(\psi) = NX^2\theta^0_{w,pm}(\psi_0) = NX^2\theta^0_{w,pm}(X\psi), \tag{19}$$

and the retention curve for bio-amended soils may finally be written as

$$\theta_{tot}(\psi, M_{bio}) = \theta_{w,bio}(\psi, M_{bio}) + NX^2\theta^0_{w,pm}(X\psi) + \theta_{r,bio}(M_{bio}) + \theta_{r,pm}. \tag{20}$$

Assuming that the effective porosity of the system has not changed or is known, the continuity equation

$$\phi_{ef} = \theta_{w,bio}(\psi, M_{bio}) + \theta_{w,pm}(\psi = 0) \tag{21}$$

must be fulfilled, the following relationship is therefore satisfied

$$NX^2 = 1 - \frac{\theta_{w,bio}(\psi, M_{bio})}{\phi_{ef}}, \tag{22}$$

and the tube-reduction factor X becomes

$$X(\psi, M_{bio}) = \sqrt{\frac{\phi_{ef} - \theta_{w,bio}(\psi, M_{bio})}{N\phi_{ef}}}. \tag{23}$$

Note that when both X and NX^2 approach 1 the impact of biofilm is negligible. However, as the values of $\theta_{w,bio}$ and/or N increase, the water retention curve in (20) differs more and more from that of the biofilm-free soil.

Several considerations about this model should be made. The existence of a constant X regardless of tube size means that biofilms proliferates in pores of all sizes. The amount of biomass in each tube is proportional to its squared radius and therefore the higher amounts of biomass are found in the larger tubes. These large tubes probably act as preferential paths through which nutrients may travel easily, promoting high growth rates. But at the same time, they also involve high velocities and high detachment effects [*Thullner and Baveye*, 2008], and are more likely to be exposed to drying periods [*Bundt et al.*, 2001]. Despite the flow limitations in smaller pores, growth is still expected because some nutrients can be available through diffusion. Moreover, the potential entrapping of suspended biomass on pore throats [*Vandevivere et al.*, 1995] may lead to additional accumulation in small tubes. On the other hand, the use of the parameters N and M_{bio} may allow to better simulate the influence of the bioaccumulation since some mechanisms that were not

considered in previous models are now introduced. Using N, a complex biofilm structure not exclusively attached to the soil grains but lying in the middle of pores is described. It is worth noting that such an architecture is probably a product of the environmental conditions and that such conditions and therefore N are spatially heterogeneous and temporally variable. However, we considered it as a fitting parameter since further research is needed to relate N to measurable/estimable properties. Finally, despite M_{bio} can be measured more or less accurately, the quantification of its impact on pore space presents some difficulties, requiring the use of approaches or indirect estimations as the equations defined above.

3.2. Relative Permeability of Bio-amended Soils

Despite the simplifications inherent in the BCC-based models, we propose a simple formulation to examine the impact that a PSSICO biofilm has on the relative permeability curve. The hydraulic conductivity of a bio-amended soil is evaluated by combining the pore-size distribution with the HagenPoiseuille equation for laminar flow, which determines that the flow rate in a tube (Q_{tube}) is proportional to the fourth power of its radius [*Alaoui et al.*, 2011; *Thullner and Baveye*, 2008],

$$Q_{tube}(r) = \bigtriangledown h \frac{\gamma_w \pi}{8\mu_w} r^4, \tag{24}$$

where $\bigtriangledown h$ is the hydraulic head gradient. Following *Thullner and Baveye* [2008], when a biomass layer of thickness δ coats the tube walls (24) is transformed to

$$Q_{tube+bio}(r) = \bigtriangledown h \frac{\gamma_w \pi}{8\mu_{bio}} \Big[[r+\delta]^4 - r^4[1-\lambda_\mu] \Big]. \tag{25}$$

Nevertheless, the permeable biofilm coats all the tubes including those larger than R, which are devoid of open-pore water according to (14). The total flow rate may be

obtained by limiting the flow contribution to the area between r and $r+\delta$ so that

$$Q_{bio}(r) = \bigtriangledown h \frac{\gamma_w \pi}{8\mu_{bio}} \Big[[r+\delta]^4 + r^4 - 2r^2[r+\delta]^2 \Big]. \tag{26}$$

It is worth noting that for values of $N > 1$ there is no symmetry around the central axis of the tubes (recall Figure 4), ruling out the possibility of using (25,26) directly. To overcome this problem we treat the entities separately (Figure 5). Since the areas are preserved, it follows that

$$N\pi[r+\delta]^2 = \pi r_0^2, \tag{27}$$

being the relations between radii

$$r + \delta = \frac{r_0}{\sqrt{N}} = \frac{r}{X\sqrt{N}}. \tag{28}$$

The total flow rate in soil may be written as

$$\begin{aligned} q_{soil}(\psi) &= -K_s k_r \bigtriangledown h = \int_{R_{min}}^{R} Q_{tube+bio}(r) f(r) dr + \int_{R}^{R_{max}} Q_{bio}(r) f(r) dr \\ &= \int_{R_{0,min}}^{R_0} Q_{tube+bio}(Xr_0) N f(r_0) dr_0 + \int_{R_0}^{R_{0,max}} Q_{bio}(Xr_0) N f(r_0) dr_0, \end{aligned} \tag{29}$$

where K_s is the real saturated hydraulic conductivity and k_r the relative permeability. Finally, substituting (25) and (26) into (29), we obtain

$$k_r(\psi) = \frac{\left[\frac{N^{-1} + N(\lambda_\mu - 1)X^4}{\lambda_\mu}\right] \int_{X\psi_{max}}^{X\psi} \frac{1}{\psi_0^2} \frac{d\theta_{w,pm}^0}{d\psi_0} d\psi_0 + \left[\frac{N^{-1} + (N-2)X^4}{\lambda_\mu}\right] \int_{X\psi}^{X\psi_{min}} \frac{1}{\psi_0^2} \frac{d\theta_{w,pm}^0}{d\psi_0} d\psi_0}{\int_{\psi_{max}}^{\psi_{min}} \frac{1}{\psi_0^2} \frac{d\theta_{w,pm}^0}{d\psi_0} d\psi_0}, \tag{30}$$

which under saturated conditions or when $X = 0$ may be rewritten as

$$k_r(\psi) \equiv \frac{N^{-1} + N(\lambda_\mu - 1)X^4}{\lambda_\mu}. \tag{31}$$

Note that despite the fact that λ_μ and X are suction-dependent parameters, both can be moved out of the integrals in (30) since the suction is constant in the equation.

4. Comparison with Experimental Data

The hypotheses assumed during the derivations were tested against two different data sets reported in the literature. Table 2 lists the physical properties of water that were used in the analysis.

In the first data set [*Rosenzweig et al.*, 2012] a sandy soil (Hamra) was artificially mixed with xanthan. Theoretically, the use of such a methodology keeps the holding characteristics of the EPS and avoids dealing with the presence of live bacteria. The mass fractions in the xanthan-soil mixture were 0.25% and 1% in dry weight, equivalent to $3.91 \cdot 10^{-3}$ and $1.576 \cdot 10^{-2}$ g EPS/cm^3 of soil. The SWRC were obtained for a large range of suctions (between 0 and 5000 cm). Results showed that the more biomass and lower suctions the larger the soil water retention. At saturation, water contents increased about 6% and 24% for the respective fractions, attributed to the swelling forces in EPS.

The second data set employed [*Rubol et al.*, 2014] considered a natural and heterogeneous soil affected by a real bioclogging process. After 12 weeks of continuous infiltration of synthetic water a complex microbial colony proliferated. Specialization of bacteria to the nutrient availability made possible the occurrence of microbial activity in all tank depths [see *Freixa et al.*, 2016, for details]. The weighted (spatially-averaged) amount of biofilm compounds at days 3 and 83 dictated the initial and final biological stages. Using the soil density and a mass of a bacterium of $9.3 \cdot 10^{-13}$ g [from *Roane et al.*, 2009], the grams of bacteria per cm^3 of soil were estimated to increase from $5.501 \cdot 10^{-5}$ to $1.574 \cdot 10^{-3}$ throughout the experiment. Similarly, the content of EPS was $8.621 \cdot 10^{-5}$ and $1.03 \cdot 10^{-4}$ grams of EPS per cm^3 of soil (by simple analogy, we used the physical characteristics of xanthan). Therefore, the total mass of biofilm (sum of bacteria and EPS) underwent more

than a ten-fold increase. For convenience, given that the initial M_{bio} was very small, we considered the relative increase instead of the absolute numbers. Thus the total biofilm proliferation was $1.536 \cdot 10^{-3}$ g biofilm/cm^3, equivalent to a biomass fraction in soil of about 0.1%. A global rise of the water held was also noticed. The weighted mean of the water content at saturation increased by 6%. Design limitations restricted the induced suctions between 100 and -100 cm.

These two experiments revealed significant displacements of the SWRC towards higher saturations (Figure 6). The hydraulic parameters of these soils are summarized in Table 1. In general terms, θ_s and θ_r increase with the amount of biomass, and α does the opposite. However, even though n is closely related to the pore-size distribution, a direct pattern was not observed.

Figure 6 compares the aforementioned experiments with the BCC-PSSICO model and two other models. First is the macroscopic model of *Rockhold et al.* [2002], that does not represent the actual distribution and morphology of the biofilm, and further neglects shrinking and swelling capacity. Consequently, results show a poor fit with this model, which is seen to require a substantial amount of biomass to obtain noticeable changes in the SWRC. Even then, fit is still not good because moisture at low suctions decrease proportionally to the amount of microbial phase (slightly observed at the bottom of the Figure 6, left). Second, the linear superposition model [*Rosenzweig et al.*, 2012] does take into account the capacity of the biofilm to retain variable amounts of water. This model results from direct superposition of the original soil and the xanthan characteristics. Surprisingly, despite this model is not process-based, a relatively good match is observed in the Rosenzweig‘s soil data. This denotes that the macroscopic water retention properties

of biofilms itself may reproduce changes under certain conditions. However, the same model cannot reproduce the event observed in Rubol's soil.

The use of mechanistically-based models allows us to better understanding processes and obtain good approaches in a wider range of situations. In this line, it is worth mentioning the works of *Rosenzweig et al.* [2009, 2014]. The study of different scenarios revealed the importance of biofilm distribution. Similar that in *Rockhold et al.* [2002], results obtained are conditioned by the presence of solids in biofilms, which was neglected in our model. This effect seems to be significant at large biofilm saturations, albeit it may be masked by other processes such as the change in soil porosity. Results from scenarios in *Rosenzweig et al.* [2009] lay far from data points because the authors neglected the effect of suction on biofilms (results not shown). Thus, despite it is beyond the scope of this study, it would be interesting to extend the model by reformulating (17) according to other pore-scale distribution patterns.

It is worth noting that the BCC-PSSICO model provides a good fit to the Rosenzweig's soil data even when the simplest $N = 1$ model is considered. Data is also well reproduced by the linear superposition model for a wide range of suctions. This indicates that when no spatial competition between water phases occurs, the SWRC may be effectively reproduced by using macroscopic models. To obtain the best fit between to the observations, we used inverse modeling calibration based on the Levenberg-Marquardt algorithm for nonlinear regression. Through calibration, our model is able to fit the changes even in the heterogeneous soil. The voids and channels observed in Figure 1 support the large N values estimated. However, differences between the two data sets are strikingly large. We hypothesize that the mechanical mixing employed in *Rosenzweig et al.* [2012] may

not reproduce the proper architecture of a biofilm, but this hypothesis still needs further confirmation in additional studies. In general terms, N is linked to the actual and historical environmental conditions surrounding biofilm, such as the flow rate and the substrate conditions [supported by *Kim et al.*, 2010; *Thullner*, 2010]. Such a intricate morphologies are a beneficial strategy because they reduce the shear stresses (flow) while increasing the diffusion of nutrients (exchange surface). This is quite a clear evidence that models should incorporate complex geometries instead of a simple one consisting of a layer attached to the tube walls.

5. Impact of Bioclogging on the Soil Hydraulic Properties

5.1. Impact of Bioclogging on the SWRC

The sensitivity of the SWRC to the parameters N and M_{bio} is illustrated in Figures 7 and 8. To simplify, we took the soil hydraulic parameters from the biofilm-free soil from *Rubol et al.* [2014] and neglected the effect of bacteria (only EPS was considered). Despite different combinations of the parameters may produce similar SWRC, substantial differences are observed in the distribution of water in pore-matrix or in biofilms. On the one hand, it should be pointed out that the choice of N does not affect the biofilm volume but its structure, giving rise to changes in the pore-size distribution. The density of small tubes increases with N. Thus, more pores are filled with water at each given suction. Such a mechanism can be so strong that may even convert the holding capacity of a sandy soil into a clay-like soil, regardless of the quantity of biomass. This way, even small amounts of biofilm may fully modify water partitioning leading to significant changes in soil properties. On the other hand, M_{bio} leads to changes in the moisture content based on the amount of water retained in both the biofilm bodies and in the modified pore-matrix. The presence of

biofilm is at the expense of the free-space available. Such a phenomenon can be observed specially at low suctions, where $\theta_{w,pm}$ becomes very small or even disappears. Therefore, the amount of water held by the biofilms (directly or indirectly) is determined by the microbial mass, its architecture, and its capacity to shrink/swell.

5.2. Impact of Bioclogging on Permeability

Figure 9 shows the relative permeability of a biofilm-free and five bio-amended soils. In principle, permeability should decrease when suction rises due to the shrinkage of the area available for water flow. However, dealing with complex biofilms requires further attention because the accumulation of biomass reshapes the pore-matrix in such a way that the overall flow capacity is affected. In general, the hydraulic conductivity of soils drops when clogging occurs because flow paths become blocked to some extent. Such a phenomenon admits further clarification due to the utilization of physical-based parameters in the model. On the one hand, the permeability of soils tends to decrease as the structural complexity of biofilm rises, related to the significance of the tube radius in (24). As a result, the presence of even small amounts of biofilm may cause a significant impact on k_r (note the drop when $N \gg 1$). On the other hand, the specific contribution of biofilm bodies to flow depends mostly on how its conductance is defined in (6) and (7).

In order to highlight the role of N and M_{bio}, μ_{bio} is first defined as constant, ignoring the effect of swelling in viscosity (Figure 9, top). The definition of a fully-permeable ($\lambda_\mu = 1$), semi-permeable or impermeable biofilm ($\lambda_\mu = \infty$) brings about significant changes in the overall permeability of the medium. On the other hand, when biofilm behaves like an impermeable body, clogging most likely occurs. In general, the larger the value of N and M_{bio} the more significant the permeability drop. However, it is worth mentioning

the opposite effect occurring for complex biofilm architectures (expressed by large N). Even though the contribution of the biofilm bodies is zero, the simple increase in open-pore water at high suctions may lead to a permeability rise. On the other hand, highly conductive biofilms induce a clear increase of the flow capacity of soils for a wide range of suctions. The effect of suction changes in λ_μ presents little but significant characteristics that make the difference (Figure 9, bottom). k_r is a result of the balance between the expressions for the biofilm volume changes in (4) and its permeability in (7).

A comparison of results to experimental data can hardly provide conclusive information because clogging effects reported in the literature poorly correlate with the amount of biomass. On the one hand, experimental studies reported hydraulic conductivity reductions ranging from one [e.g., *Rubol et al.*, 2014; *Volk et al.*, 2016; *Zhong and Wu*, 2013] to a few orders of magnitude [e.g., *Engesgaard et al.*, 2006; *Or et al.*, 2007b; *Taylor and Jaffé*, 1990; *Vandevivere and Baveye*, 1992b]. Although relevant data under unsaturated conditions is scarce, the recent work of *Volk et al.* [2016] provided detailed direct measurements in which permeability was reduced by a factor of four. On the other hand, the models of permeability in unsaturated soils are so far quite limited. Even though a few approaches constituted a great advance in modeling [e.g., *Mostafa and Van Geel*, 2007; *Rosenzweig et al.*, 2009] we believe that the capacity of bio-amended soils to let water through is not properly treated. In this line, our model does include a complex (and realistic) representation of biofilm that is capable of predicting permeability reductions of distinct orders of magnitude, similar to the ones found in the literature. Results show that the permeability of bio-amended soils is a function of the biofilm conductance and of the distribution of phases (open-pore water and biofilm) in the tube cross-sections, with

a certain emphasis on the biofilm architecture (N). The more complex characterization of biofilms is at the expense of the pore space definition. Despite of that the pore interconnectivity is required to reflect the complexity of the multidimensional flow in real porous media, a simple analysis using our model already provides a rough estimation of the relative permeability at some intermediate scale. The number of parameters studied and the need to define the flow through pore interconnections hamper determining whether such a simplification over- or underpredicts the real impact on soils. The lack of knowledge on this point together with the uncertainties illustrated in Figure 9 underline the need of further research.

Despite the importance of the transport of nutrients for biofilm growth, and the mobilization of contaminants in many fields, we consider it to be out of the scope of this paper. Here, we just state that the geometries discussed above also entail consequences in transport, as the interfaces through which mass is exchanged are redefined, modifying the exposure, nutrients availability, and removal rates.

6. Conclusions

The growth of biofilm in soils exerts a strong influence on hydraulic parameters, modifying the shape of the water retention curve and the relative permeability. We present a model that aims at improving our understanding of such a phenomenon. Our approach consists in modeling the local characteristics of soil as an ensemble of capillary tubes of different diameters. This simple (and widely used in biofilm-free soils) methodology is extended by the incorporation of a biofilm composed of bacterial cells and EPS. Three main points are considered: i) biofilm alone is capable of holding large amounts of water and has particular hydraulic properties; ii) microbial phase undergoes changes in volume; and

iii) biofilm is not a convex surface but a channeled complex geometry (which allows us to redefine the concept of tubes that are colonized by a biofilm with complex geometries). On the basis of these points, the new properties of the bio-colonized soil are derived yielding a set of analytical equations that account for the spatial competition between open-pore water and biofilm at pore-scale. First, the incorporation of channeled biofilm bodies that shrink/swell enables us to obtain a new pore-size distribution from which the soil-water retention curve is derived. Subsequently, the geometrical distribution of a permeable biofilm in tubes provides an approach to relative permeability. Such a flexible framework can incorporate with no effort other type of hypotheses regarding biofilm characteristics and distribution. Assumptions based on the tube theory vastly underestimate pore singularities, simplifying its geometry and interconnections and possibly underpredicting water content distribution and flow rates. The current model can be understood as a tool to isolate and better study the local impact of biofilms on the hydraulic properties.

The new expression for the SWRC is evaluated by the data of three bio-amended soils. The model can properly reproduce the displacement of the SWRC towards higher saturations. Moreover, a sensitivity analysis on both the SWRC and the relative permeability functions is performed in order to understand the role of the parameters presented. From it, we could explain how even small amounts of biofilm may fully reshape the pore network leading to significant changes in hydraulic properties. Results indicate that the morphology, the spatial distribution of biomass and the EPS swelling and shrinking characteristics are key factors controlling the properties of bio-amended soils. The number of hypotheses included in the model enhances the need for a sound analysis of these properties of

biofilms, as they play a major role in the overall soil behavior and therefore they should be included somehow in biofilm modeling.

Acknowledgments. The research leading to these results has received funding from the European Union FP7 under grant agreement no 619120 (Demonstrating Managed Aquifer Recharge as a Solution to Water Scarcity and Drought MARSOL), and PCOFUND-GA-2008-226070. Additional support was provided by the Spanish Ministry of Economy and Competitiveness (project SCARCE, ref. CSD2009-00065), and the Ministry of Science and Innovation (project FEAR, ref. CGL2012-38120; and the research fellowship FPI BES-2013-063419). XS acknowledges support from the ICREA Academia Program. We would like to thank three anonymous reviewers and the associate editor for their constructive comments. We also thank George von Knorring for reviewing the English of an early version of the manuscript. Data can be requested by contacting the corresponding author.

References

Abdel-Waly, A. (2013), Laboratory Study On Activating Indigenous Microorganisms to Enhance Oil Recovery, *Journal of Canadian Petroleum Technology*, *38*(02), doi: 10.2118/99-02-05.

Alaoui, A., J. Lipiec, and H. H. Gerke (2011), A review of the changes in the soil pore system due to soil deformation: A hydrodynamic perspective, *Soil and Tillage Research*, *115-116*, 1–15, doi:10.1016/j.still.2011.06.002.

Baveye, P., P. Vandevivere, B. L. Hoyle, P. C. DeLeo, and D. S. de Lozada (1998), Environmental Impact and Mechanisms of the Biological Clogging of Saturated Soils and

493 Aquifer Materials, *Critical Reviews in Environmental Science and Technology*, *28*(2),
494 123–191, doi:10.1080/10643389891254197.

495 Beckett, C., and C. Augarde (2013), Prediction of soil water retention properties using
496 pore-size distribution and porosity, *Canadian Geotechnical Journal*, *450*(April), 435–
497 450, doi:10.1139/cgj-2012-0320.

498 Billings, N., A. Birjiniuk, T. S. Samad, P. S. Doyle, and K. Ribbeck (2015), Material
499 properties of biofilmsa review of methods for understanding permeability and mechanics,
500 *Reports on Progress in Physics*, *78*(3), 036,601, doi:10.1088/0034-4885/78/3/036601.

501 Bozorg, A., I. D. Gates, and A. Sen (2015), Using bacterial bioluminescence to evaluate
502 the impact of biofilm on porous media hydraulic properties, *Journal of Microbiological*
503 *Methods*, *109*, 84–92, doi:10.1016/j.mimet.2014.11.015.

504 Brooks, R. H., and A. T. Corey (1964), Hydraulic properties of porous media, *Hydrology*
505 *papers Colorado State University*, *3*.

506 Bundt, M., F. Widmer, M. Pesaro, J. Zeyer, and P. Blaser (2001), Preferential flow paths:
507 Biological 'hot spots' in soils, *Soil Biology and Biochemistry*, *33*(6), 729–738.

508 Burdine, N. (1953), Relative Permeability Calculations From Pore Size Distribution Data,
509 doi:10.2118/225-G.

510 Carsel, R., and R. Parrish (1988), Developing joint probability distributions of soil water
511 retention characteristics, *Water Resources Research*, *24*(5), 755–769.

512 Castegnier, F., N. Ross, R. P. Chapuis, L. Deschênes, and R. Samson (2006), Long-term
513 persistence of a nutrient-starved biofilm in a limestone fracture., *Water research*, *40*(5),
514 925–34, doi:10.1016/j.watres.2005.12.038.

Chenu, C. (1993), Clay-or sand-polysaccharide associations as models for the interface between micro-organisms and soil: water related properties and microstructure, *Geoderma*, *56*(1-4), 143–156.

Christensen, T. H., P. L. Bjerg, S. A. Banwart, R. Jakobsen, G. Heron, and H.-J. Albrechtsen (2000), Characterization of redox conditions in groundwater contaminant plumes, *Journal of Contaminant Hydrology*, *45*(3-4), 165–241.

Clement, T., B. Hooker, and R. Skeen (1996), Macroscopic models for predicting changes in saturated porous media properties caused by microbial growth, *Groundwater*, *34*(5), 934–942.

Cooke, R., and I. D. Kuntz (1974), The properties of water in biological systems, *Annual Review of Biophysics and Bioengineering*, *3*, 95–126, doi: 10.1146/annurev.bb.03.060174.000523.

Cunningham, A., R. Gerlach, L. Spangler, and A. Mitchell (2009), Microbially enhanced geologic containment of sequestered supercritical CO2, *Energy Procedia*, *1*(1), 3245–3252, doi:10.1016/j.egypro.2009.02.109.

Cunningham, A. B., w. G. Characklis, F. Abedeen, and D. Crawford (1991), Influence of biofilm accumulation on porous media hydrodynamics, *Environmental Science and Technology*, *25 (7)*, 1305–1311.

Davit, Y., H. Byrne, J. Osborne, J. Pitt-Francis, D. Gavaghan, and M. Quintard (2013), Hydrodynamic dispersion within porous biofilms, *Physical Review E - Statistical, Nonlinear, and Soft Matter Physics*, *87*(1), 24–29, doi:10.1103/PhysRevE.87.012718.

De Beer, D., and A. Schramm (1999), Micro-environments and mass transfer phenomena in biofilms studied with microsensors, in *Water Science and Technology*, vol. 39, pp.

538 173–178, doi:10.1016/S0273-1223(99)00165-1.

539 de Gennes, P.-G. (1979), *Scaling Concepts in Polymer Physics*, Cornell University Press.

540 De Muynck, W., N. De Belie, and W. Verstraete (2010), Microbial carbonate precip-

541 itation in construction materials: A review, *Ecological Engineering*, *36*(2), 118–136,

542 doi:10.1016/j.ecoleng.2009.02.006.

543 DeJong, J., K. Soga, and E. Kavazanjian (2013), Biogeochemical processes and geotechni-

544 cal applications: progress, opportunities and challenges, *Géotechnique*, *63*(4), 287–301.

545 Donlan, R. M. (2002), Biofilms: Microbial life on surfaces, doi:10.3201/eid0809.020063.

546 Dupin, H. J., P. K. Kitanidis, and P. L. McCarty (2001), Pore-scale modeling of biological

547 clogging due to aggregate expansion: A material mechanics approach, *Water Resources*

548 *Research*, *37*(12), 2965–2979, doi:10.1029/2001WR000306.

549 Ehrlich, H. L. (1999), Microbes as Geologic Agents: Their Role in Mineral Formation,

550 *Geomicrobiology Journal*, *16*(2), 135–153, doi:10.1080/014904599270659.

551 Engesgaard, P., D. Seifert, and P. Herrera (2006), Bioclogging in porous media: tracer

552 studies, in *Riverbank Filtration Hydrology*, vol. 60, pp. 93–118, Springer Netherlands.

553 Ezeuko, C., A. Sen, A. Griogoryan, and G. I.D. (2011), Pore-network modeling of biofilm

554 evolution in porous media, *Biotechnology and Bioengineering*, *108*(10), 2413–2423, doi:

555 10.1002/bit.23183.

556 Fenchel, T. (2002), Microbial behavior in a heterogeneous world, *Science*, *296*(5570),

557 1068–1071, doi:10.1126/science.1070118.

558 Flemming, H.-C., and J. Wingender (2010), The biofilm matrix, *Nature reviews. Micro-*

559 *biology*, *8*(9), 623–33, doi:10.1038/nrmicro2415.

Freixa, A., S. Rubol, A. Carles-Brangarí, D. Fernàndez-Garcia, A. Butturini, X. Sanchez-Vila, and A. M. Romaní (2016), The effects of sediment depth and oxygen concentration on the use of organic matter : An experimental study using an in fi ltration sediment tank, *Science of the Total Environment*, *540*, 20–31, doi:10.1016/j.scitotenv.2015.04.007.

Hand, V. L., J. R. Lloyd, D. J. Vaughan, M. J. Wilkins, and S. Boult (2008), Experimental studies of the influence of grain size, oxygen availability and organic carbon availability on bioclogging in porous media, *Environmental Science & Technology*, *42*(5), 1485–1491.

Kennedy, P. L., and P. J. Van Geel (2001), Impact of density on the hydraulics of peat filters, *Canadian Geotechnical Journal*, *38*, 1213–1219, doi:10.1139/t01-047.

Kim, J., H. Choi, and Y. Pachepsky (2010), Biofilm morphology as related to the porous media clogging, *Water Research*, *44*(4), 1193–1201, doi:10.1016/j.watres.2009.05.049.

Laspidou, C. S., and B. E. Rittmann (2004), Modeling the development of biofilm density including active bacteria, inert biomass, and extracellular polymeric substances, *Water Research*, *38*(14-15), 3349–3361, doi:10.1016/j.watres.2004.04.037.

Lawrence, J. R., D. R. Korber, B. D. Hoyle, J. W. Costerton, and D. E. Caldwell (1991), Optical sectioning of microbial biofilms, *Journal of Bacteriology*, *173*, 6558–6567.

Likos, W., and R. Jaafar (2013), Pore-scale model for water retention and fluid partitioning of partially saturated granular soil, *Journal of Geotechnical and Geoenvironmental Engineering*, *139*(5), 724–737, doi:10.1061/(ASCE)GT.1943-5606.0000811.

Mauclaire, L., A. Schürmann, and F. Mermillod-Blondin (2006), Influence of hydraulic conductivity on communities of microorganisms and invertebrates in porous media: a case study in drinking water slow sand filters, *Aquatic Sciences*, *68*(1), 100–108, doi:

583 10.1007/s00027-005-0811-4.

584 Mitchell, J. K., and K. Soga (2005), Soil Composition and Engineering Properties, in
585 *Fundamentals of Soil Behavior*, pp. 83–108, CBS Publishers & Distributors Pvt. Ltd.

586 Morris, R. H., M. I. Newton, P. R. Knowles, M. Bencsik, P. A. Davies, P. Griffin, and
587 G. McHale (2011), Analysis of clogging in constructed wetlands using magnetic reso-
588 nance, *The Analyst*, *136*, 2283–2286, doi:10.1039/c0an00986e.

589 Mostafa, M., and P. Van Geel (2012), Validation of a Relative Permeability Model for Bio-
590 clogging in Unsaturated Soils, *Vadose Zone Journal*, *11*(1), doi:10.2136/vzj2011.0044.

591 Mostafa, M., and P. J. Van Geel (2007), Conceptual Models and Simulations for
592 Biological Clogging in Unsaturated Soils, *Vadose Zone Journal*, *6*(1), 175, doi:
593 10.2136/vzj2006.0033.

594 Mualem, Y. (1976), A new model for predicting the hydraulic conductivity of unsaturated
595 porous media, *Water Resources Research*, *12*(3).

596 Or, D., B. Smets, and J. Wraith (2007a), Physical constraints affecting bacterial habitats
597 and activity in unsaturated porous mediaa review, *Advances in Water Resources*, *30*(6-
598 7), 1505–1527.

599 Or, D., S. Phutane, and A. Dechesne (2007b), Extracellular polymeric substances affecting
600 pore-scale hydrologic conditions for bacterial activity in unsaturated soils, *Vadose Zone*
601 *Journal*, *6*(2), 298–305, doi:10.2136/vzj2006.0080.

602 Pedretti, D., M. Barahona-Palomo, B. Diogo, D. Fernàndez-Garcia, X. Sanchez-Vila,
603 and D. M. Tartakovsky (2012), Probabilistic analysis of maintenance and operation
604 of artificial recharge ponds, *Advances in Water ...*, *36*(April 2011), 23–35, doi:
605 10.1016/j.advwatres.2011.07.008.

606 Peña-Cabriales, J. J., and M. Alexander (1979), Survival of Rhizobium in Soils
607 Undergoing Drying, *Soil Science Society of America Journal*, *43*(5), 962, doi:
608 10.2136/sssaj1979.03615995004300050030x.

609 Picioreanu, C., J. Xavier, and M. van Loosdrecht (2004), Advances in mathematical
610 modeling of biofilm structure, *Biofilms*, *1*(4), 337–349, doi:10.1017/S1479050505001572.

611 Pintelon, T. R. R., C. Picioreanu, M. C. M. van Loosdrecht, and M. L. Johns (2012),
612 The effect of biofilm permeability on bioclogging of porous media, *Biotechnology and*
613 *Bioengineering*, *109*(4), 1031–1042, doi:10.1002/bit.24381.

614 Qin, C.-Z., and S. M. Hassanizadeh (2015), Pore-Network Modeling of Solute Transport
615 and Biofilm Growth in Porous Media, *Transport in Porous Media*, *110*(3), 345–367,
616 doi:10.1007/s11242-015-0546-1.

617 Rebata-Landa, V., and J. C. Santamarina (2012), Mechanical Effects of Biogenic Nitrogen
618 Gas Bubbles in Soils, doi:10.1061/(ASCE)GT.1943-5606.0000571.

619 Rittmann, B. (1993), The significance of biofilms in porous media, *Water Resources Re-*
620 *search*, *29*(7), 2195–2202.

621 Roane, T. M., K. A. Reynolds, R. M. Maier, and I. L. Pepper (2009), *Environmental*
622 *Microbiology*, 9–36 pp., Elsevier, doi:10.1016/B978-0-12-370519-8.00002-X.

623 Rockhold, M., R. Yarwood, M. Niemet, P. Bottomley, and J. Selker (2002), Considerations
624 for modeling bacterial-induced changes in hydraulic properties of variably saturated
625 porous media, *Advances in Water Resources*, *25*(5), 477–495.

626 Rodríguez-Escales, P., A. Folch, B. M. van Breukelen, G. Vidal-Gavilan, and X. Sanchez-
627 Vila (2016), Modeling long term Enhanced in situ Biodenitrification and induced hetero-
628 geneity in column experiments under different feeding strategies, *Journal of Hydrology*,

538, 127–137, doi:10.1016/j.jhydrol.2016.04.012.

Rosenzweig, R., U. Shavit, and A. Furman (2009), The influence of biofilm spatial distribution scenarios on hydraulic conductivity of unsaturated soils, *Vadose Zone Journal*, *8*(4), 1080, doi:10.2136/vzj2009.0017.

Rosenzweig, R., U. Shavit, and A. Furman (2012), Water retention curves of biofilm-affected soils using xanthan as an analogue, *Soil Science Society of America Journal*, *76*(1), 61–69, doi:10.2136/sssaj.

Rosenzweig, R., A. Furman, and U. Shavit (2013), A channel network model as a framework for characterizing variably saturated flow in biofilm-affected soils, *Vadose Zone Journal*, *12*(2), doi:10.2136/vzj2012.0079.

Rosenzweig, R., A. Furman, C. Dosoretz, and U. Shavit (2014), Modeling biofilm dynamics and hydraulic properties in variably saturated soils using a channel network model, *Water Resources Research*, *50*, 5678–5697, doi:10.1002/ 2013WR015211.

Ross, N., R. Villemur, L. Deschênes, and R. Samson (2001), Clogging of a limestone fracture by stimulating groundwater microbes, *Water Research*, *35*, 2029–2037, doi:10.1016/S0043-1354(00)00476-0.

Rubol, S., A. Freixa, A. Carles-Brangarí, D. Fernàndez-Garcia, A. M. Romaní, and X. Sanchez-Vila (2014), Connecting bacterial colonization to physical and biochemical changes in a sand box infiltration experiment, *Journal of Hydrology*, *517*, 317–327, doi:10.1016/j.jhydrol.2014.05.041.

Samsó, R., and J. García (2014), The Cartridge Theory: a description of the functioning of horizontal subsurface flow constructed wetlands for wastewater treatment, based on modelling results., *The Science of the Total Environment*, *473-474*, 651–8,

doi:10.1016/j.scitotenv.2013.12.070.

Seki, K., T. Miyazaki, and M. Nakano (1998), Effects of microorganisms on hydraulic conductivity decrease in infiltration, *European Journal of Soil Science*, *49*(2), 231–236.

Selker, J. S., J. T. McCord, and C. K. Keller (1999), *Vadose Zone Processes*, 352 pp., CRC Press.

Soleimani, S., P. J. Van Geel, O. B. Isgor, and M. B. Mostafa (2009), Modeling of biological clogging in unsaturated porous media, *Journal of Contaminant Hydrology*, *106*(1-2), 39–50, doi:10.1016/j.jconhyd.2008.12.007.

Stewart, P. S. (2012), Mini-review: convection around biofilms., *Biofouling*, *28*(2), 187–98, doi:10.1080/08927014.2012.662641.

Stoodley, P., D. DeBeer, and Z. Lewandowski (1994), Liquid flow in biofilm systems, *Applied and Environmental Microbiology*, *60*(8), 2711–2716.

Stoodley, P., K. Sauer, D. G. Davies, and J. W. Costerton (2002), Biofilms as complex differentiated communities., *Annual review of microbiology*, *56*, 187–209, doi:10.1146/annurev.micro.56.012302.160705.

Tamaru, Y., Y. Takani, T. Yoshida, and T. Sakamoto (2005), Crucial role of extracellular polysaccharides in desiccation and freezing tolerance in the terrestrial cyanobacterium Nostoc commune, *Applied and Environmental Microbiology*, *71*(11), 7327–7333, doi:10.1128/AEM.71.11.7327-7333.2005.

Taylor, S. W., and P. R. Jaffé (1990), Biofilm growth and the related changes in the physical properties of a porous medium: 1. Experimental investigation, *Water Resources Research*, *26*(9), 2153–2159, doi:10.1029/WR026i009p02153.

674 Taylor, S. W., P. Milly, and P. R. Jaffe (1990), Biofilm Growth and the Related Changes in
675 the Physical Properties of a Porous Medium. 2. Permeability, *Water Resources Research*
676 *WRERAQ,*, *26*(9).
677 Thullner, M. (2010), Comparison of bioclogging effects in saturated porous media within
678 one-and two-dimensional flow systems, *Ecological Engineering*, *36*(2), 176–196, doi:
679 10.1016/j.ecoleng.2008.12.037.
680 Thullner, M., and P. Baveye (2008), Computational pore network modeling of the influence
681 of biofilm permeability on bioclogging in porous media, *Biotechnology and Bioengineer-*
682 *ing*, *99*(6), 1337–1351, doi:10.1002/bit.21708.
683 Van Cuyk, S., R. Siegrist, A. Logan, S. Masson, E. Fischer, and L. Figueroa (2001),
684 Hydraulic and purification behaviors and their interactions during wastewater treat-
685 ment in soil infiltration systems, *Water Research*, *35*, 953–964, doi:10.1016/S0043-
686 1354(00)00349-3.
687 van Genuchten, M. T. (1980), A closed-form equation for predicting the hydraulic con-
688 ductivity of unsaturated soils, *Soil science society of America Journal*, *44*(5).
689 Vandevivere, P., and P. Baveye (1992a), Saturated Hydraulic Conductivity Reduction
690 Caused by Aerobic Bacteria in Sand Columns, *Soil Science Society of America Journal*,
691 *56*, 1–13, doi:10.2136/sssaj1992.03615995005600010001x.
692 Vandevivere, P., and P. Baveye (1992b), Effect of bacterial extracellular polymers on the
693 saturated hydraulic conductivity of sand columns, *Applied and Environmental Micro-*
694 *biology*, *58*(5), 1690–1698.
695 Vandevivere, P., P. Baveye, D. Sanchez de Lozaa, and P. DeLeo (1995), Microbial clogging
696 of saturated soils and aquifer materials: Evaluation of mathematical models, *Water*

Resources Research, *31*(9), 2173–2180.

Volk, E., S. C. Iden, A. Furman, W. Durner, and R. Rosenzweig (2016), Biofilm effect on soil hydraulic properties: Experimental investigation using soil-grown real biofilm, *Water Resources Research*, pp. 1–20, doi:10.1002/2016WR018866.

Wagner, M., D. Taherzadeh, C. Haisch, and H. Horn (2010), Investigation of the mesoscale structure and volumetric features of biofilms using optical coherence tomography., *Biotechnology and bioengineering*, *107*(5), 844–53, doi:10.1002/bit.22864.

Wilking, J. N., T. E. Angelini, A. Seminara, M. P. Brenner, and D. a. Weitz (2011), Biofilms as complex fluids, *MRS Bulletin*, *36*(05), 385–391, doi:10.1557/mrs.2011.71.

Yarwood, R., M. Rockhold, M. Niemet, J. Selker, and P. Bottomley (2006), Impact of microbial growth on water flow and solute transport in unsaturated porous media, *Water Resources Research*, *42*(10), doi:10.1029/2005WR004550.

Young, I. M., and J. W. Crawford (2004), Interactions and self-organization in the soil-microbe complex., *Science*, *304*, 1634–1637, doi:10.1126/science.1097394.

Zhang, T. C., Y. Fu, P. L. Bishop, M. Kupferle, S. FitzGerald, H. H. Jiang, and C. Harmer (1995), Transport and biodegradation of toxic organics in biofilms, *Journal of Hazardous Materials*, *41*, 267–285, doi:10.1016/0304-3894(94)00118-Z.

Zhong, X., and Y. Wu (2013), Bioclogging in porous media under continuous-flow condition, *Environmental Earth Sciences*, *68*(8), 2417–2425, doi:10.1007/s12665-012-1926-2.

Figure 1. Images of biofilms showing heterogeneous structure. Left: mature biofilm forming voids and channels between two soil grains [modified from *Hand et al.*, 2008]. Right: Stained EPS and bacteria developed on a steel surface [modified from *Donlan*, 2002].

Figure 2. Estimate of λ_μ due to changes in the water content of the biofilm caused by swelling/shrinking processes, based on (7).

Figure 3. Solid (mineral), biofilm, water and air phases present in a bio-amended soil under variably suction stress. Left: distribution of the different phases within the total volume. Right: cross-sections of the capillary tubes, displaying the spatial distribution of air, open-pore water and water in biofilm. For each suction value, only the tubes (of the newly defined pore-matrix) smaller than R remain fully saturated while the others have the specific amount of water relative to the volume of biofilm they content.

Figure 4. Sketch showing how N modifies the pore-size distribution of the porous medium. This has a direct impact on the volumetric water content. The top scenario depicts the behavior of a biofilm-free soil whereas the others reproduce the changes in the distribution of phases with N. $\theta_{w,bio}$ and ψ remain constant in all cases.

Figure 5. Sketch of the geometrical distribution of biofilm and its impact upon flow. The permeability approach requires a slight modification of the geometry. Symmetry around the central axis is recovered while the areas of the phases are still conserved. Left: A tube of radius r_0 is redefined as a tube of radius $r + \delta$ for mathematical convenience. Right: a single tube of radius r_0 is transformed into four new pore-matrix tubes ($N = 4$) of radius $r + \delta$. Green areas are microbial phase cross-sections through which water flows. When $r > R$ (left case), despite flow is not allowed through the pore-matrix, the microbial phase does contribute to flow.

.

Figure 6. Comparison of bioclogging models with experimental data reported by *Rosenzweig et al.* [2012], left figure, and *Rubol et al.* [2014], right figure. The bioclogging models presented include the BCC-PSSICO model, the macroscopic model of *Rockhold et al.* [2002] and the linear superposition model by *Rosenzweig et al.* [2012].

Figure 7. Effect of N on the water holding capacities of the composite medium (left, in black), distinguishing between water in the pore-matrix (middle, in brown) and pure biofilm (right, in green). The mass fraction of EPS is assumed equal to $5{\cdot}10^{-3}$ g EPS/cm^3 in order to isolate the effect of N.

Figure 8. Effect of M_{bio} on the volumetric water content for $N = 1$ (top) and $N = 10$ (bottom), distinguishing between water in the pore-matrix (middle, in brown) and pure biofilm (right, in green). The mass of biofilm is expressed in g EPS/cm^3.

Figure 9. Effect of different combinations of N, and M_{bio} on the relative permeability for soils. Lines correspond to the biofilm-free soil (red line), and five theoretical bio-amended soils. The mass of biofilm is expressed in g EPS/cm^3. Top: the dynamic viscosity of water flowing through biofilms is considered as constant. Regardless of the swelling status, biofilm is defined as impermeable ($\lambda_\mu = \infty$), semi-permeable ($\lambda_\mu = 5$), or fully-permeable ($\lambda_\mu = 1$). Bottom: the parameter accounting for the viscosity changes when biofilm shrinks/swells is evaluated.

Table 1. Parameters of the van Genuchten model and of the amount of biomass. SWRC parameters are obtained from *Rosenzweig et al.* [2012] and using a nonlinear regression on data from *Rubol et al.* [2014]. θ_r in Rubol's soil is evaluated using a linear superposition equation based on the weighted average of the grain-size fractions and hydraulic parameters in *Carsel and Parrish* [1988]. The biological parameters are the estimated values of bacteria, EPS and total biofilm.

Soil	Biomass [%]	ϕ_{ef} [-]	θ_r [-]	n [cm^{-1}]	α [-]	ρ_s [g/cm^3]	M_{bact} [g/cm^3]	M_{EPS} [g/cm^3]	M_{bio} [g/cm^3]
Rosenzweig	0	0.402	0.026	2.32	0.042	1.56	0	0	0
Rosenzweig	0.25	0.420	0.048	2.11	0.031	-	0	$3.91 \cdot 10^{-3}$	$3.91 \cdot 10^{-3}$
Rosenzweig	1	0.480	0.054	1.89	0.022	-	0	$1.576 \cdot 10^{-2}$	$1.576 \cdot 10^{-2}$
Rubol	0	0.207	0.044	1.63	0.087	1.5	0	0	0
Rubol	0.1	0.222	0.045	2.18	0.029	-	$1.519 \cdot 10^{-3}$	$1.683 \cdot 10^{-5}$	$1.536 \cdot 10^{-3}$

Table 2. Physical properties of water.

σ	$\cos(\beta)$	γ_w	ρ_w	μ_w
$[N/cm]$	[-]	$[N/cm^3]$	$[g/cm^3]$	$[sN/cm^2]$
$7.15 \cdot 10^{-4}$	1	$9.789 \cdot 10^{-3}$	0.998	$1.002 \cdot 10^{-7}$

Figure 1.

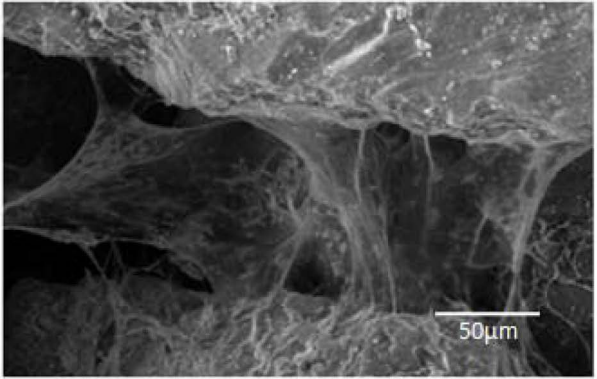
50µm

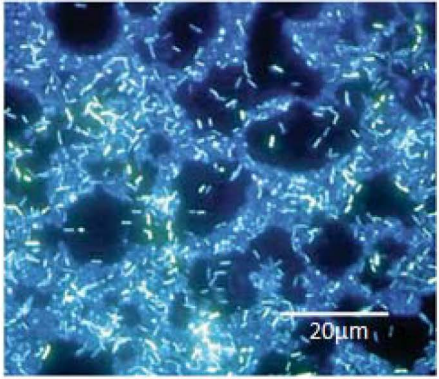
20µm

Figure 2.

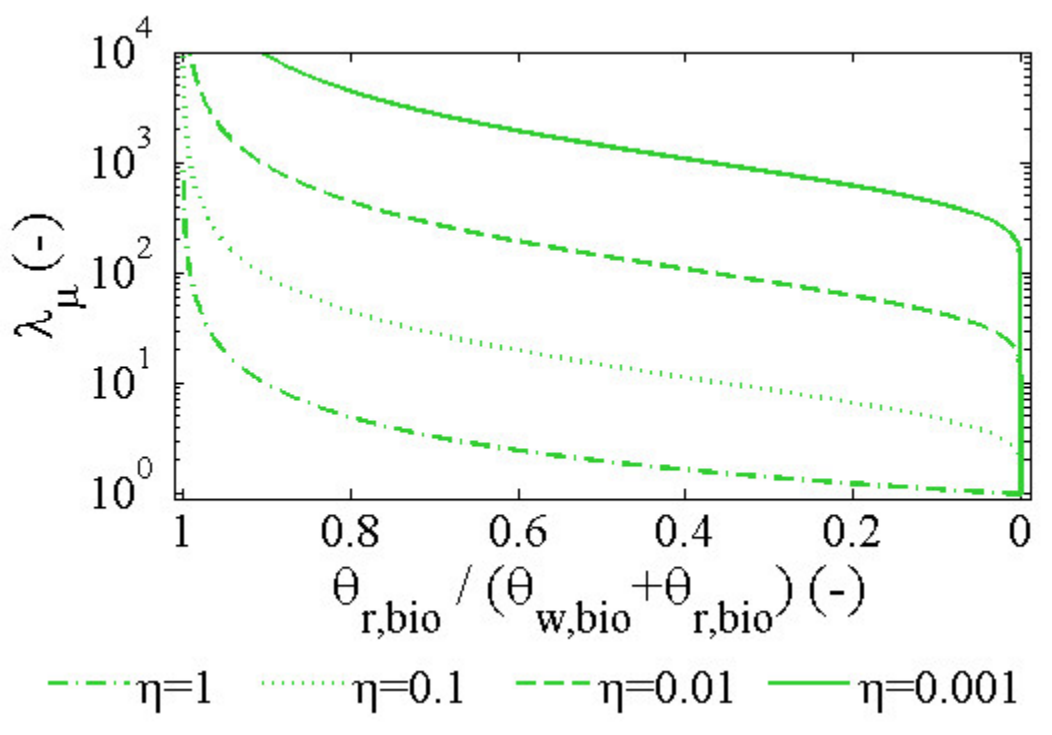
10^4
10^3
10^2
10^1
10^0
λ_μ (-)
1
0.8
0.6
0.4
0.2
0
$\theta_{r,bio} / (\theta_{w,bio} + \theta_{r,bio})$ (-)
η=1
η=0.1
η=0.01
η=0.001

Figure 3.

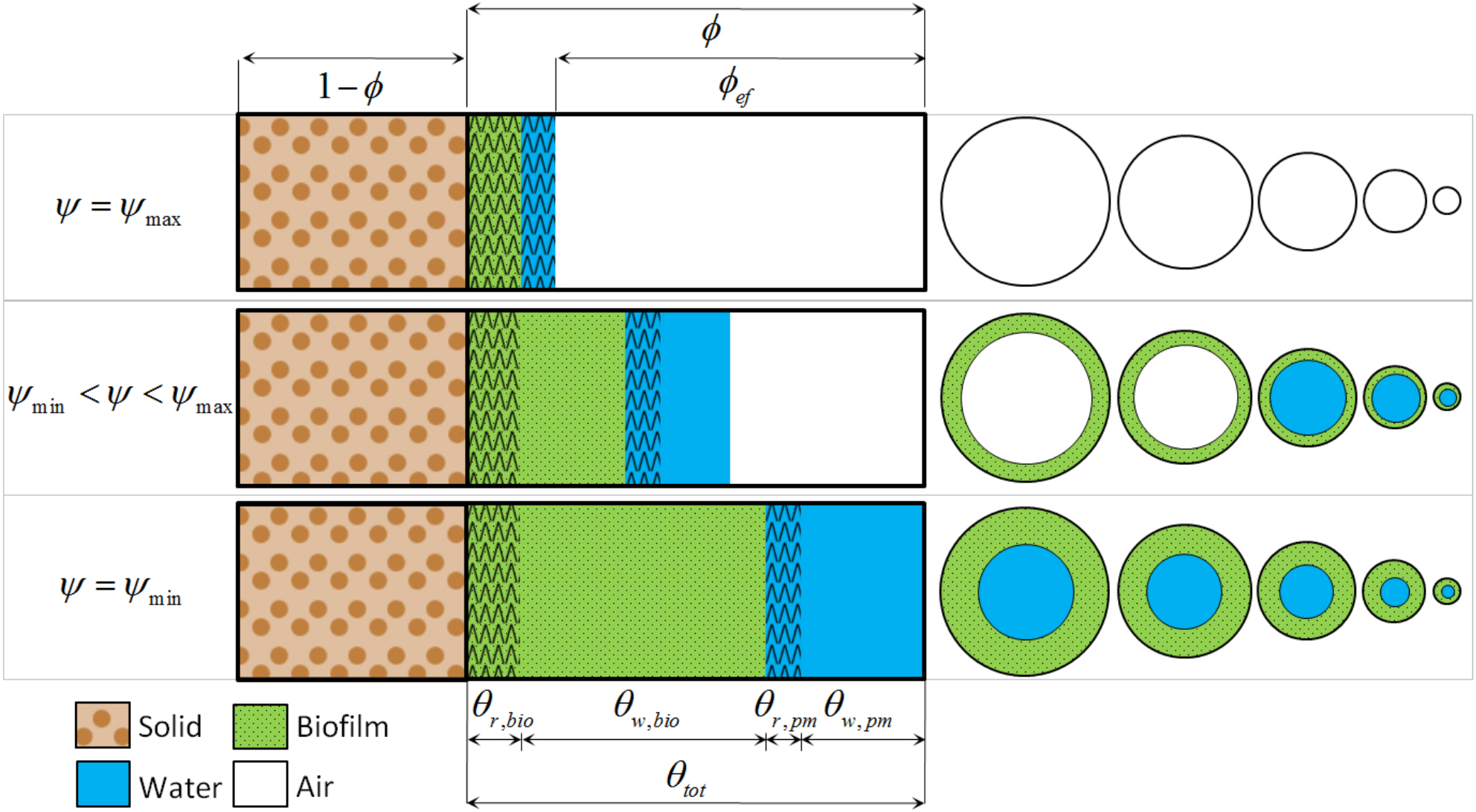
ϕ
$1-\phi$
ϕ_{ef}
$\psi = \psi_{max}$
$\psi_{min} < \psi < \psi_{max}$
$\psi = \psi_{min}$
Solid
Biofilm
Water
Air
$\theta_{r,bio}$
$\theta_{w,bio}$
$\theta_{r,pm}$
$\theta_{w,pm}$
θ_{tot}

Figure 4.

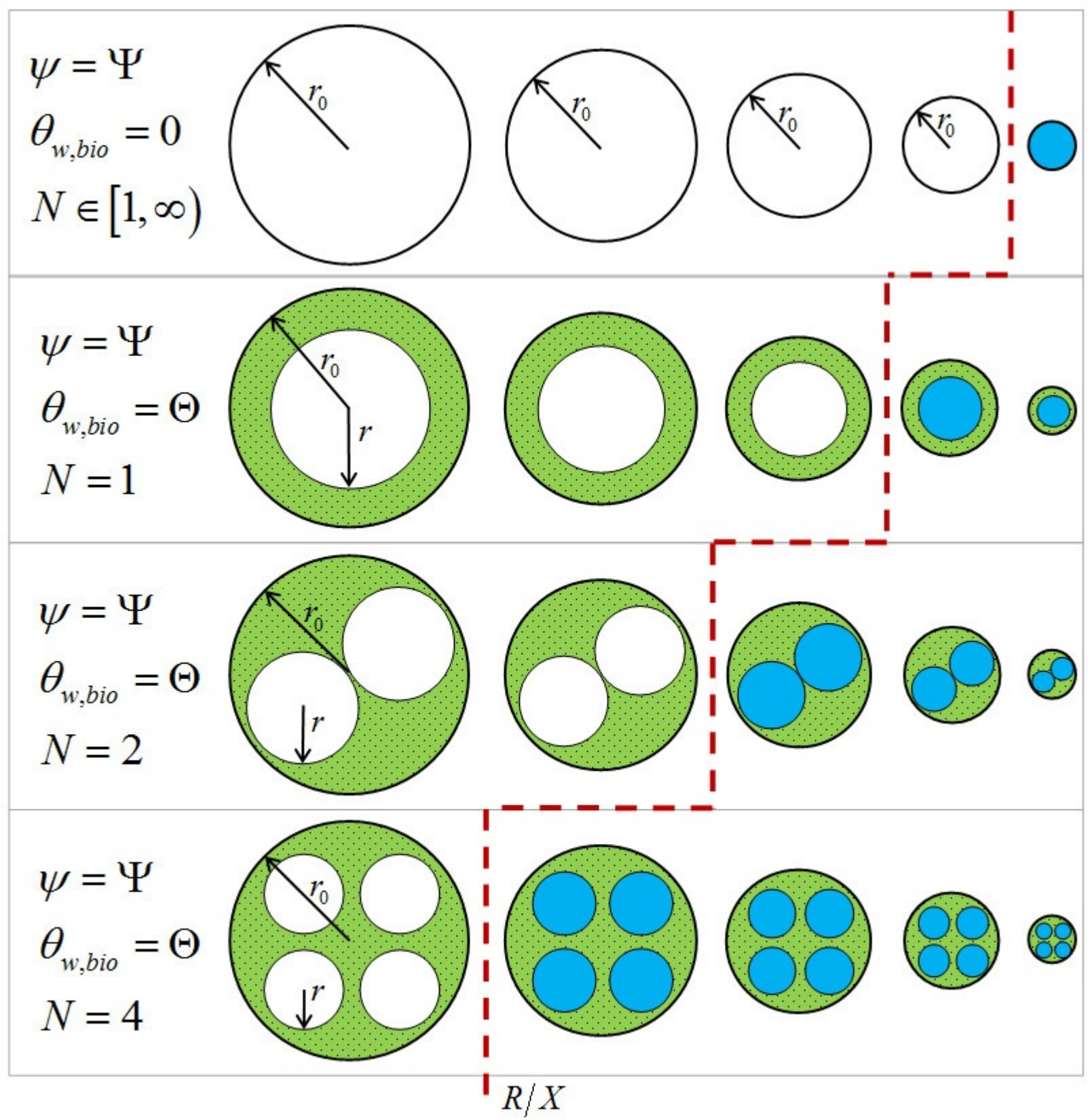
$\psi = \Psi$
$\theta_{w,bio} = 0$
$N \in [1, \infty)$
r_0
$\psi = \Psi$
$\theta_{w,bio} = \Theta$
$N = 1$
r_0
r
$\psi = \Psi$
$\theta_{w,bio} = \Theta$
$N = 2$
r_0
r
$\psi = \Psi$
$\theta_{w,bio} = \Theta$
$N = 4$
r_0
r
R/X

Figure 5.

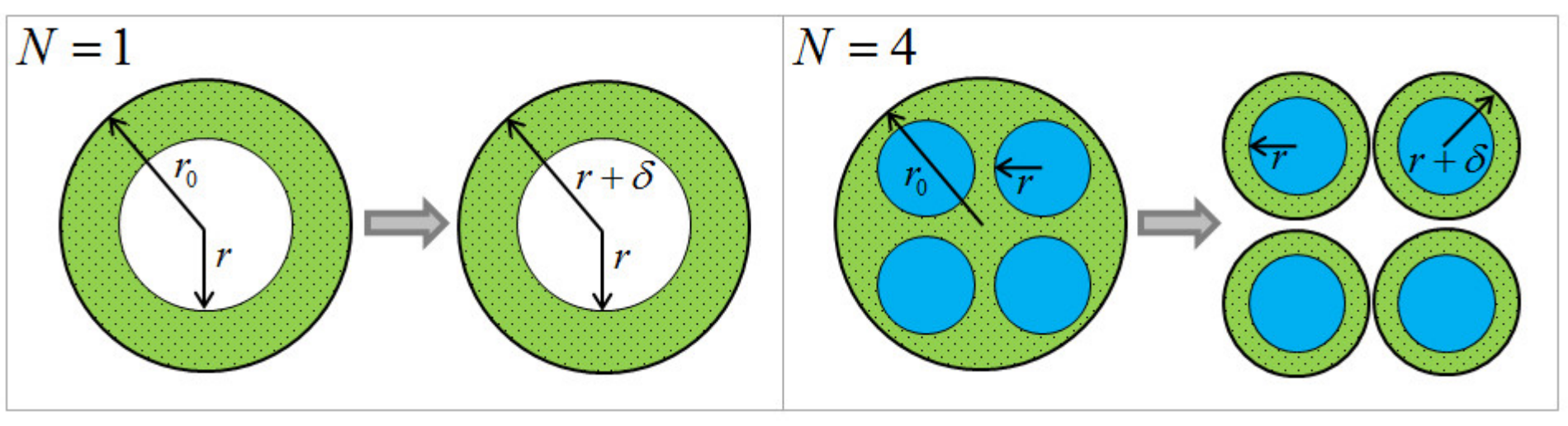
N = 1
r0
r
r + δ
r
N = 4
r0
r
r
r + δ

Figure 6.

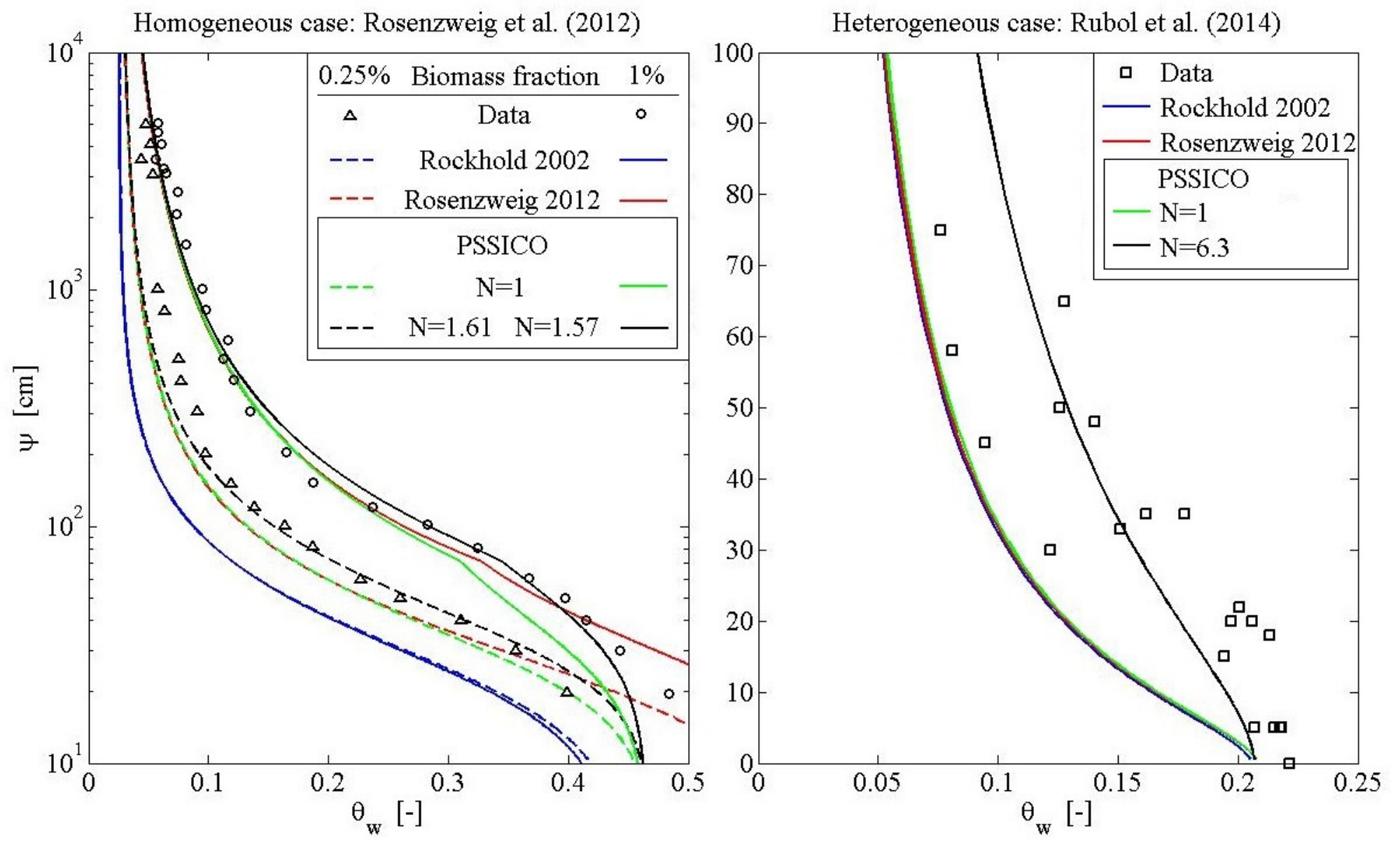
Homogeneous case: Rosenzweig et al. (2012)
Heterogeneous case: Rubol et al. (2014)
0.25% Biomass fraction 1%
Data
Rockhold 2002
Rosenzweig 2012
PSSICO
N=1
N=1.61 N=1.57
N=6.3
ψ [cm]
θw [-]

Figure 7.

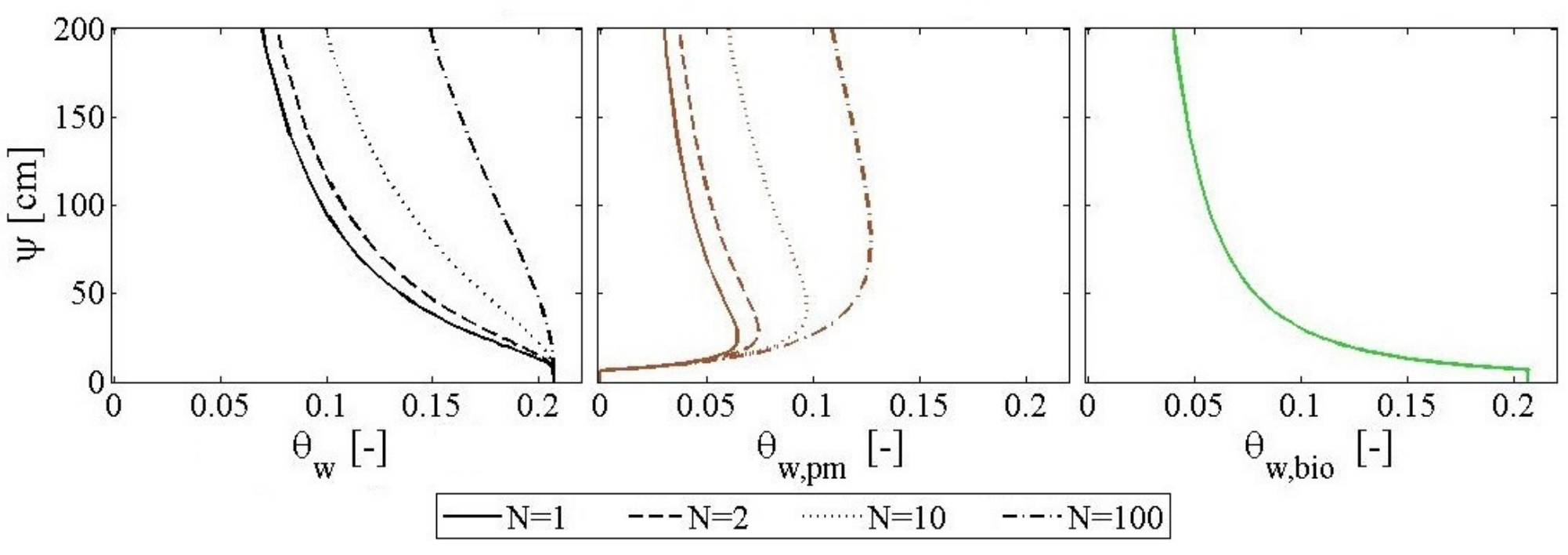
200
150
100
50
0
ψ [cm]
0
0.05
0.1
0.15
0.2
θw [-]
θw,pm [-]
θw,bio [-]
N=1
N=2
N=10
N=100

Figure 8.

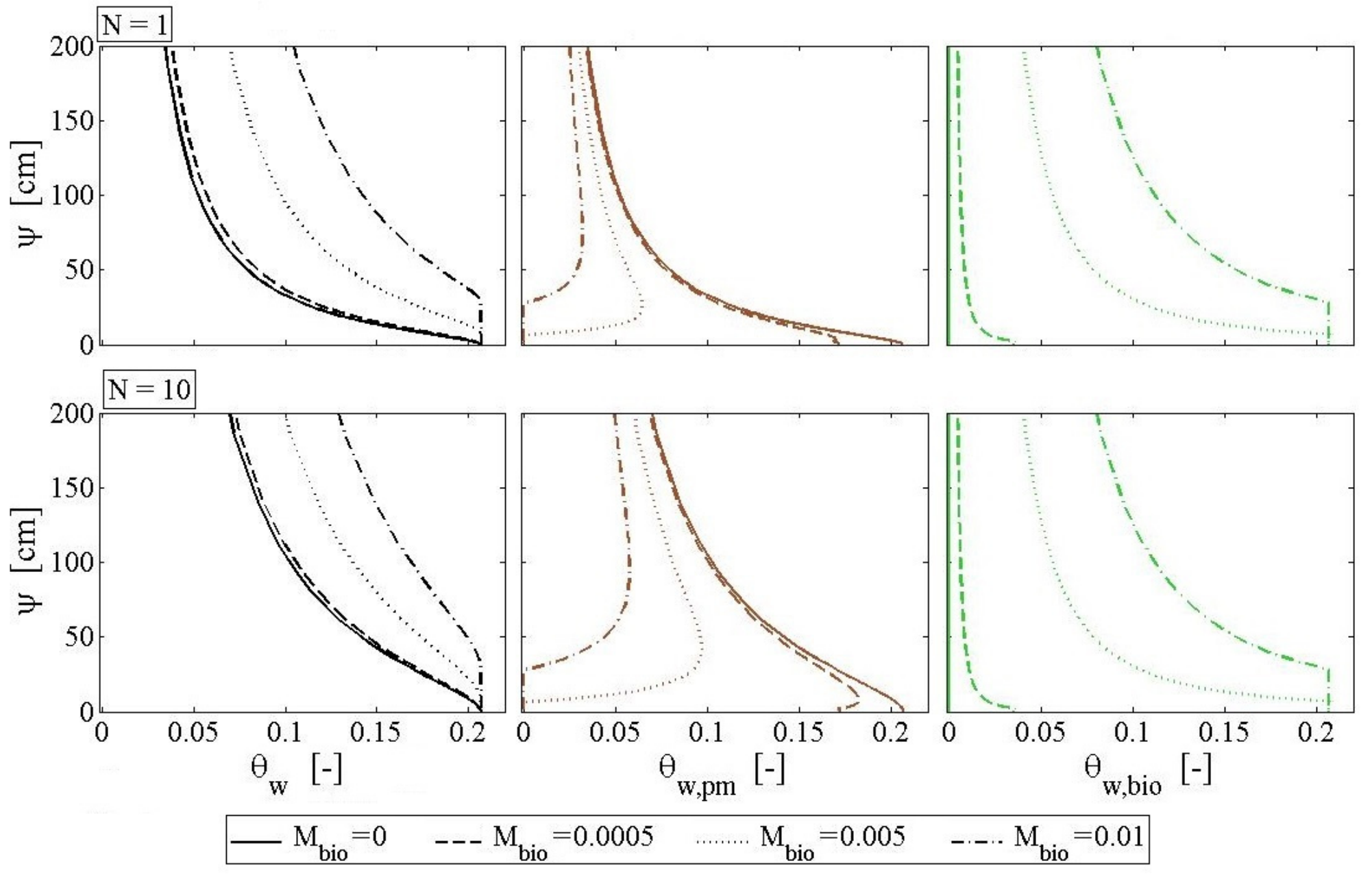
N = 1
N = 10
ψ [cm]
200
150
100
50
0
0
0.05
0.1
0.15
0.2
θw [-]
θw,pm [-]
θw,bio [-]
Mbio =0
Mbio =0.0005
Mbio =0.005
Mbio =0.01

Figure 9.

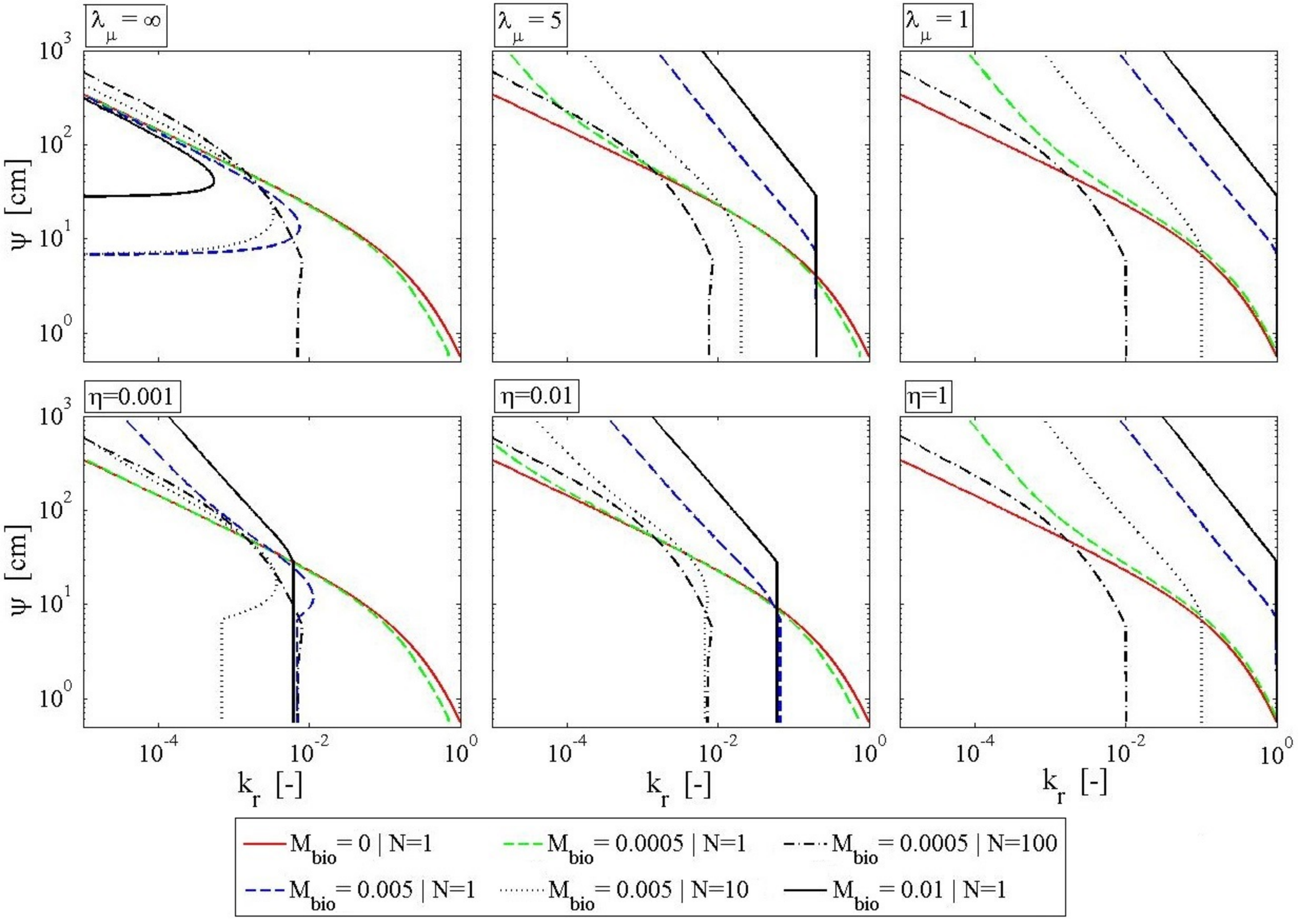
λμ = ∞
λμ = 5
λμ = 1
η=0.001
η=0.01
η=1
ψ [cm]
kr [-]
10^3
10^2
10^1
10^0
10^-4
10^-2
10^0
Mbio = 0 | N=1
Mbio = 0.0005 | N=1
Mbio = 0.0005 | N=100
Mbio = 0.005 | N=1
Mbio = 0.005 | N=10
Mbio = 0.01 | N=1